Antarct. Meteorite Res., **12**, 168–182, 1999

TRACE ELEMENT DISTRIBUTIONS IN YAMATO-793605, A CHIP OFF THE "MARTIAN LHERZOLITE" BLOCK

Meenakshi WADHWA[1], Gordon A. MCKAY[2] and Ghislaine CROZAZ[3]

[1] *Department of Geology, The Field Museum, Roosevelt Rd. at Lake Shore Dr., Chicago, IL 60605, U.S.A.*
[2] *NASA Johnson Space Center, SN4, Houston, TX 77058, U.S.A.*
[3] *Department of Earth and Planetary Sciences and McDonnell Center for the Space Sciences, Washington University, St. Louis, MO 63130, U.S.A.*

Abstract: *In situ* ion microprobe analyses of various phases in Yamato-793605 (Y 79) confirm that it is very similar to the other two lherzolitic shergottites, ALHA77005 and LEW88516. Differences in absolute REE abundances between bulk samples of these meteorites can be largely accounted for by sample heterogeneity. The three lherzolites were formed by essentially identical processes and they may even have originated from the same lithological unit on Mars. Preservation of major element zonation in olivines of Y79 indicates that it is less equilibrated than the other lherzolitic shergottites, and may have crystallized at shallower depth. The parent magmas of lherzolitic shergottites, like those of other shergottites, were derived by partial melting of a partly depleted martian mantle.

1. Introduction

All SNC meteorites are igneous rocks believed to have originated on Mars (MCSWEEN, 1994 and references therein) and, until there is a sample return from this planet, they are the only samples of martian crust available for laboratory studies. As such, they provide valuable insights into the geological evolution of their intriguing parent body. Currently only 13 meteorites belong to the SNC group and, therefore, any recognition of new SNC meteorites is of great interest to meteoriticists and planetary scientists.

The object of this study, the 16 g Yamato-793605 (hereon referred to as Y79) is a recent addition to the known SNCs. First classified as a diogenite, it was later correctly identified as a shergottite (YANAI, 1995), confirmed as a martian meteorite (MAYEDA *et al.*, 1995), and recognized as strikingly similar to the two lherzolitic shergottites, ALHA 77005 and LEW88516 (MIKOUCHI and MIYAMOTO, 1996). Because of its small size, the NIPR recognized the need for a consortium study, which was led by KOJIMA *et al.* (1997). This multinational effort has already led to the publication of a number of studies including aspects of this meteorite's mineralogy and petrology (IKEDA, 1997; MIKOUCHI and MIYAMOTO, 1997), chemistry (EBIHARA *et al.*, 1997; MITTLEFEHLDT *et al.*, 1997; WARREN and KALLEMEYN, 1997), descriptions of altered phases produced mainly by terrestrial weathering (IKEDA, 1997; MITTLEFEHLDT *et al.*, 1997) and various isotopic properties (EUGSTER and POLNAU, 1997; GRADY *et al.*, 1997; MISAWA *et al.*, 1997; NAGAO

et al., 1997). Most of these studies have stressed the many characteristics that are common to all three martian lherzolites.

In this paper, we present the results of *in situ* ion microprobe analyses of trace and minor element microdistributions in minerals of Y79; these analyses were made subsequent to thorough petrographic and electron microprobe documentation. Our aim is to understand the petrogenesis of this meteorite and to discuss its relationship to the other two lherzolitic shergottites. As we will show, this study also strongly supports a close association of all three lherzolites.

2. Sample Description and Analytical Methods

One thin section of Y79 (Y793605,51-4) was studied. It consists predominantly (>90%) of a poikilitic region, with sub-mm sized olivine grains enclosed within a large oikocryst (~6 mm across, composed of a zoned pigeonite grain surrounded by a rim of augite), and is similar to the "light" lithology previously described in ALHA77005 (LUNDBERG *et al.*, 1990). Y79 also has a small non-poikilitic region with smaller grains of pyroxene (mostly pigeonite), olivine, maskelynite, and opaque minerals present in regions interstitial to the poikilitic region. It is comparable to the "dark" lithology described in ALHA77005 (LUNDBERG *et al.*, 1990). X-ray mapping and mineral identification and analyses were first performed at the Johnson Space Center using a Cameca SX-100 electron microprobe. This information and additional petrologic observations were used to identify a diverse set of pyroxenes, olivines, melt inclusions, and feldspathic glass appropriate for trace element analyses. Concentrations of rare earth elements (REEs) and other selected trace and minor elements were then measured *in situ* in selected spots, using the Washington University modified CAMECA IMS-3f secondary ion mass spectrometer (SIMS). Analytical procedures for such measurements have been described in detail by ZINNER and CROZAZ (1986) and LUNDBERG *et al.* (1988).

3. Results

3.1. Petrography and electron microprobe results

Our petrographic observations support the conclusion of MIKOUCHI and MIYAMOTO (1997) that Y79 is very similar to other Antarctic martian meteorites ALHA77005 and LEW88516 (hereafter referred to as ALH and LEW, respectively). Because those workers and IKEDA (1997) have described the petrography of Y79 in detail, we will only report features that are pertinent to our SIMS study, plus some features that have not been previously described. The elemental maps in Fig. 1 show nearly the entire section Y793605,51-4. As reported by other workers (*e.g.*, MIKOUCHI and MIYAMOTO, 1997), the sample consists of a poikilitic region that occupies most of the section, and a non-poikilitic region that appears only on the extreme right side of the maps in Fig. 1. The poikilitic region consists of a large poikilitic pigeonite grain rimmed by augite. Olivine and chromite are enclosed by pigeonite and augite. Olivine in the poikilitic region contains melt inclusions, which are well described by IKEDA (1997) and MIKOUCHI and MIYAMOTO (1997). The non-poikilitic region consists of olivine, maskelynite, pigeonite, and augite.

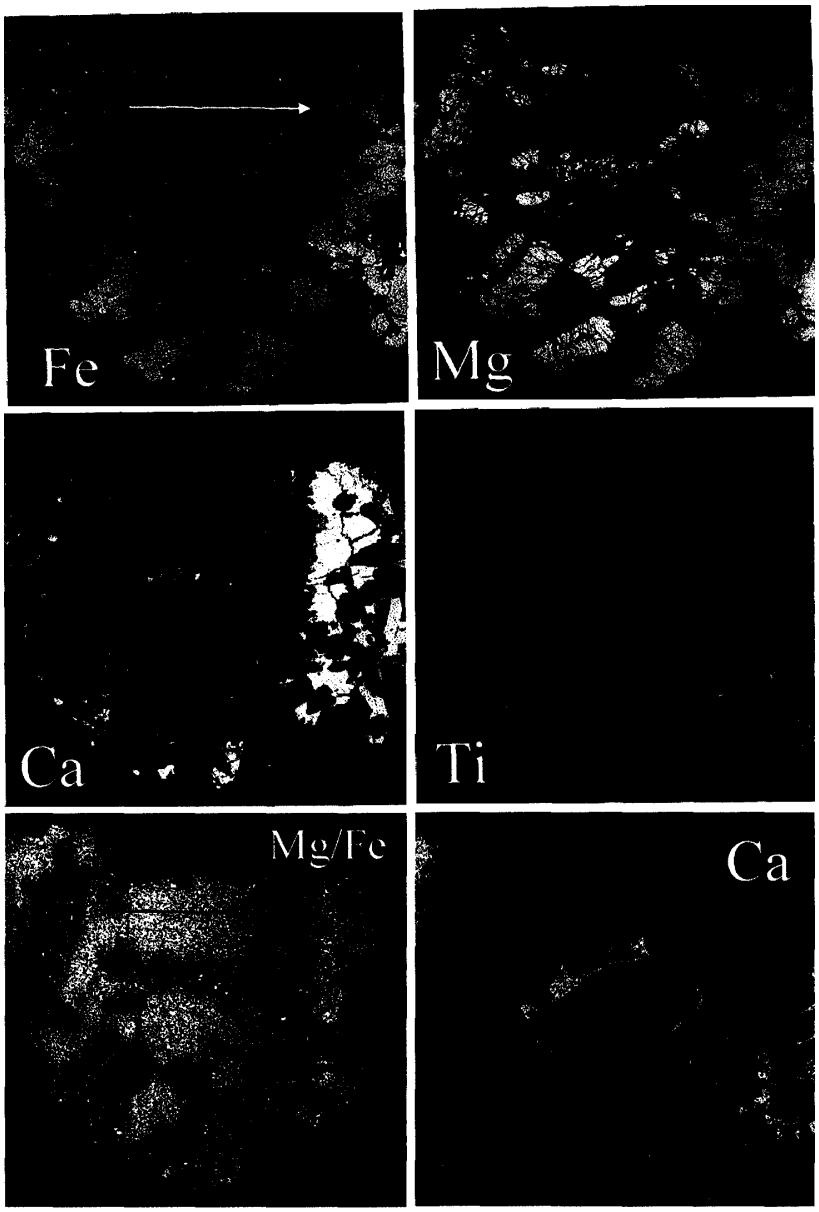

Fig. 1. Elemental maps of Y79. For all images except Ti, warmer colors indicate higher concentrations or values, with white being the highest. For the Ti image (on the right in the middle row), brighter blue indicates higher concentration. The first five images cover nearly the entire thin section, and are 6.7 mm in width. The arrows in the top and bottom images at the left show the location of the profile shown in Fig. 3. The poikilitic region occupies most of the section, with the non-poikilitic region occupying only the extreme right portion, to the right of the poikilitic augite band that runs from top to bottom (bright yellow in the Ca image). Note the zoning in the large poikilitic pigeonite crystal that occupies the major portion of the thin section, especially the Mg/Fe zoning shown in the bottom left image. The Mg/Fe image also shows zoning in individual olivine crystals enclosed in the poikilitic olivine (Fo_{67-73}). The bottom right image is 1.5 mm in width, and shows the intricate Ca zoning in poikilitic pigeonite adjacent to enclosed olivine crystals.

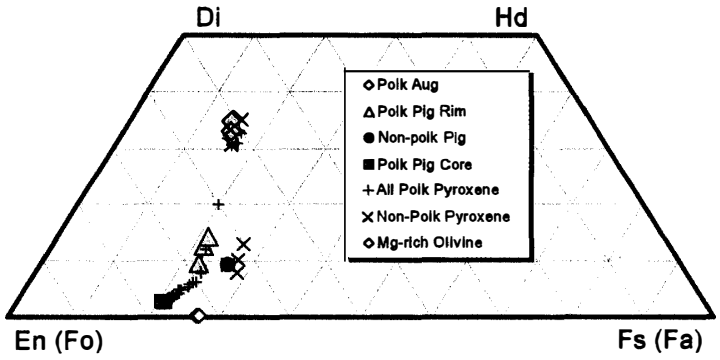

Fig. 2. Pyroxene compositions in Y79. Compositions of pyroxenes and olivines analyzed by SIMS are shown with colored symbols. Other poikilitic pyroxenes are also shown (+), as are other non-poikilitic pyroxenes (×), and are in agreement with compositions reported by previous workers (e.g., MIKOUCHI and MIYAMOTO, 1997).

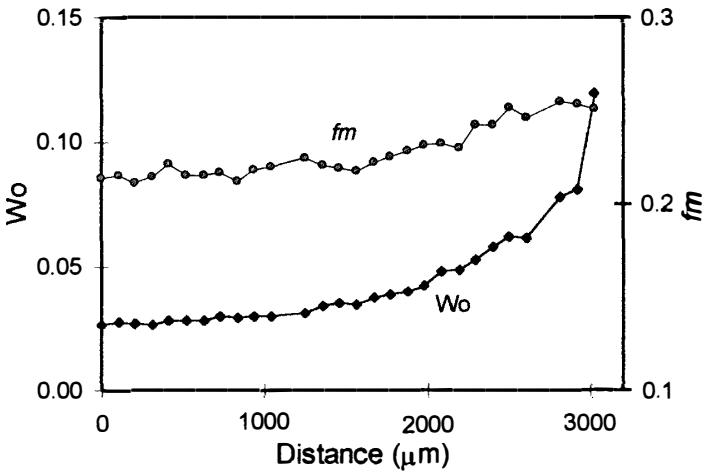

Fig. 3. Zoning profiles from core to rim in poikilitic pigeonite of Y79, along traverse shown in Fig. 1.

Our mineral analyses are in agreement with those of previous workers. Pyroxene compositions are shown in Fig. 2, which compares the major element compositions of pyroxenes we analyzed by SIMS (see Section 3.2 below) with a much larger number of analyses that represent nearly the complete range of pyroxene compositions in the sample. Poikilitic pigeonites tend to be more Mg-rich than those in the non-poikilitic region, and also extend to lower Ca contents. There is little difference in augite compositions between the poikilitic and non-poikilitic regions. Our SIMS analyses include pyroxenes that span the entire range observed in the sample.

Much of the poikilitic region consists of a single large pigeonite crystal that is zoned from core to rim, as can be seen in both the Ca map and the Mg/Fe map in Fig. 1. Core-to-rim zoning along a traverse indicated by the arrows in Fig. 1 is illustrated in Fig. 3. This zoning is smooth and continuous, and likely represents primary igneous zoning.

We observed olivines ranging from Fo_{67} to Fo_{74}, in agreement with other workers. We observed one feature not previously reported by other workers, *i.e.*, some of the

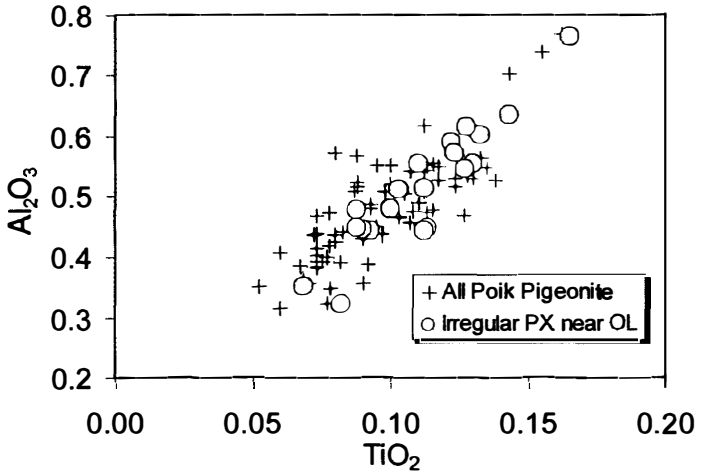

Fig. 4. Comparison of Al vs. Ti systematics of pyroxenes in smoothly zoned poikilitic crystals (e.g., Fig. 3) with pyroxenes in the irregular regions near enclosed olivine crystals (e.g., bottom right portion of Fig. 1).

poikilitically enclosed olivine grains exhibit elemental zoning within individual grains, as can be seen in Fig. 1 (in the Mg/Fe map). In fact, the olivine near the bottom of the whole-section images displays zoning that spans nearly the entire compositional range of olivines observed elsewhere in the section.

The smooth zoning pattern in the large poikilitic pyroxene is disturbed around the enclosed olivines, as can best be seen in the Ca maps in Fig. 1, especially the higher magnification image at the bottom right. These disturbances appear as "flame-shaped" regions emanating from the enclosed olivine crystals. However, the zoning trends in these "irregular" regions are indistinguishable from such trends in smoothly zoned regions. This is evident in Fig. 4 which compares Ti *vs.* Al variations for a traverse through the largest irregular region (slightly left of center in the bottom right section of Fig. 1) with such variations in all other poikilitic pyroxene analyses. We further note that this is also the case for Ca *vs.* Mg/Fe, Al *vs.* Mg/Fe, and Ca *vs.* Al systematics in these pyroxenes.

3.2. *Ion microprobe results*

In the poikilitic region, we made ion microprobe analyses on 1 olivine (Fo_{73}), 12 pigeonite, and 2 augite spots. We also measured the REE concentrations of a glassy region within a melt inclusion present in a poikilitically enclosed olivine grain. This inclusion is very similar to the inclusion shown in Fig. 1L of IKEDA (1997) and to the right inclusion in Fig. 9A of MIKOUCHI and MIYAMOTO (1997). In the non-poikilitic region, we analyzed individual grains of maskelynite (1 spot, $An_{66}Ab_{33}Or_1$), olivine (1 spot, Fo_{69}), and pigeonite (6 spots). Major element compositions of analyzed pyroxenes are shown in Fig. 2.

Figures 5 and 6 and Table 1 present representative REE abundances in minerals of Y79 (filled symbols). For comparison, REE concentrations in minerals of ALH (HARVEY *et al.*, 1993) are also shown in Figs. 5 and 6 (open symbols). Note that HREEs in maskelynite and LREEs in olivine are not included since these REEs are

Table 1. Representative rare earth element (REE) abundances (in ppb) in pyroxenes, plagioclase and olivine of lherzolitic shergottite Yamato-793605; REE concentrations (in ppm) in the glassy region of a glass-rich melt inclusion within a poikilitically enclosed olivine grain are also given. Errors are 1σ based on counting statistics only.

	Poikilitic Pigeonite (Core)	Poikilitic Pigeonite (Rim)	Poikilitic Augite (Rim)	Non-Poikilitic Pigeonite	Plagioclase	Olivine	Glass in Melt Inclusion
La	3.1 ± 0.9	10.1 ± 2.1	41.0 ± 4.9	31.2 ± 3.9	60.4 ± 2.5	n.d.	0.61 ± 0.03
Ce	39.8 ± 4.5	44.7 ± 5.0	192 ± 21	121 ± 8	116 ± 5	n.d.	1.65 ± 0.08
Pr	2.0 ± 0.6	4.8 ± 1.1	36.4 ± 5.3	20.3 ± 3.2	14.7 ± 1.1	n.d.	0.24 ± 0.01
Nd	8.8 ± 1.9	17.3 ± 3.0	259 ± 15	133 ± 10	65.5 ± 3.0	n.d.	1.46 ± 0.05
Sm	3.7 ± 2.1	24.7 ± 4.3	211 ± 16	163 ± 12	23.3 ± 2.9	n.d.	0.99 ± 0.05
Eu	1.0 ± 0.5	6.4 ± 1.2	81.4 ± 6.9	42.3 ± 4.2	401 ± 12	2.8 ± 0.5	0.40 ± 0.02
Gd	16.7 ± 2.6	63.2 ± 6.5	513 ± 43	433 ± 36	32.6 ± 3.2	11.9 ± 1.8	2.24 ± 0.10
Tb	4.1 ± 0.9	15.2 ± 1.9	134 ± 12	117 ± 12	4.3 ± 0.7	2.8 ± 0.5	0.50 ± 0.03
Dy	39.8 ± 3.5	152 ± 8	790 ± 38	920 ± 39	28.8 ± 2.0	26.4 ± 1.8	3.61 ± 0.10
Ho	11.2 ± 1.5	33.5 ± 2.9	161 ± 14	202 ± 16	n.d.*	8.0 ± 0.8	0.77 ± 0.04
Er	38.3 ± 3.3	128 ± 8	491 ± 25	661 ± 39	n.d.	33.5 ± 2.1	2.04 ± 0.07
Tm	5.3 ± 1.1	17.2 ± 2.8	59.9 ± 6.4	97 ± 7	n.d.	5.2 ± 0.7	0.29 ± 0.02
Yb	40.9 ± 4.7	138 ± 11	475 ± 30	705 ± 41	n.d.	51.8 ± 3.0	1.92 ± 0.08
Lu	9.8 ± 1.8	20.6 ± 3.3	55.5 ± 8.0	103 ± 13	n.d.	12.6 ± 1.3	0.32 ± 0.03

*n.d. = not detectable.

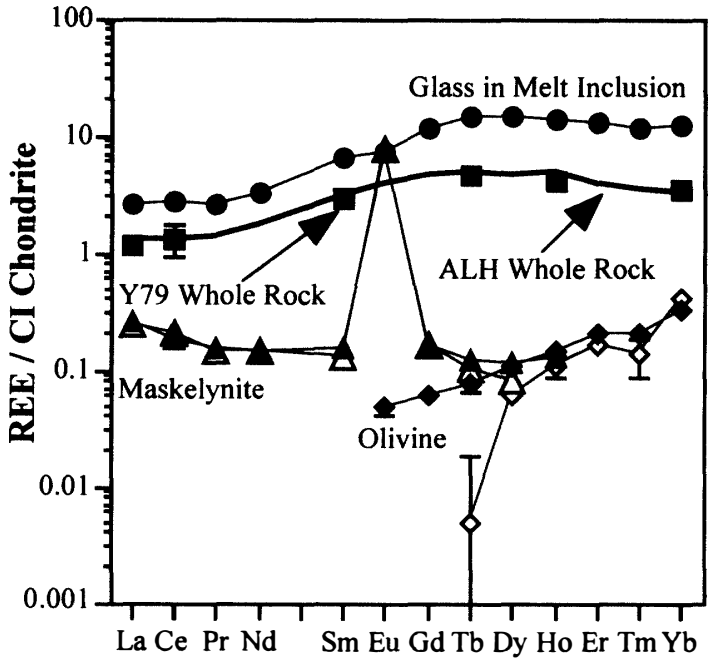

Fig. 5. REE abundances (normalized to the CI chondrite values of EBIHARA and ANDERS, 1982) in olivine, maskelynite, and glass in a melt inclusion in Y79 (solid symbols); for comparison, data for maskelynite (open triangles) and olivine (open diamonds) in ALH are also shown (HARVEY et al., 1993). Errors are 1σ from counting statistics only. Filled squares are whole rock data for Y79 (WARREN and KALLEMEYN, 1997) whereas the solid line represents whole rock data for ALH (SMITH et al., 1984).

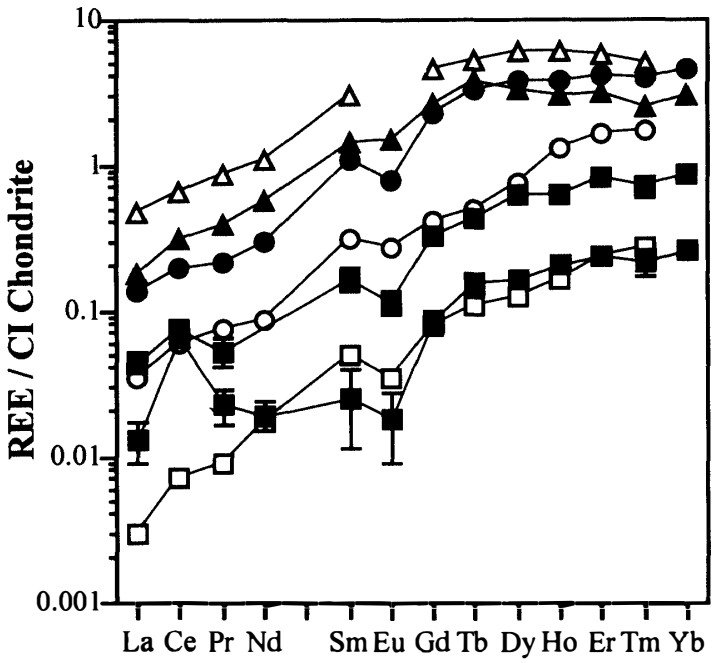

Fig. 6. Representative REE abundances (normalized to the CI chondrite values of EBIHARA and ANDERS, 1982) in pyroxenes of Y79 (solid symbols; this work) and ALH (open symbols; HARVEY et al., 1993). Errors are 1σ from counting statistics only. Squares represent low-Ca poikilitic pyroxenes; triangles high-Ca poikilitic pyroxenes; and circles low-Ca non-poikilitic pyroxenes. Note that the two REE patterns shown for low-Ca poikilitic pyroxenes in Y79 are representative of the cores (with lower REE abundances) and the rims (with higher REE abundances). REE compositions of Y79 pyroxenes shown here are also given in Table 1.

present in these minerals below the detection limit of the ion microprobe.

REE abundances in maskelynite and olivine of Y79 and ALH (Fig. 5) are the same within 2σ errors (errors plotted in Fig. 5 are 1σ from counting statistics only). Also shown in Fig. 5 are REE concentrations in a glassy area of the melt inclusion referred to above. The melt inclusion is predominantly glassy, although other minerals such as pyroxene (20–30 vol%) are also present. The REE patterns of the glass in this inclusion, the Y79 whole rock (filled squares; WARREN and KALLEMEYN, 1997) and the ALH whole rock (solid line; SMITH *et al.*, 1984) are all similar, although absolute abundances in the whole rocks are somewhat lower.

As in ALH, pyroxenes in Y79 have characteristic LREE-depleted patterns with small Eu anomalies (Fig. 6). However, there is an indication that the REE patterns of the low-Ca pyroxenes of ALH (CI-normalized Tm/La ~ 40–60) are somewhat steeper than those of Y79 (CI-normalized Tm/La < 40). In addition, five of the twelve low-Ca poikilitic pyroxenes analyzed in Y79 have positive Ce anomalies (Ce/Ce* ~ 1.5–4, where Ce* is the interpolated value between chondrite-normalized abundances of La and Pr). No Ce anomalies were found in low-Ca non-poikilitic and high-Ca poikilitic pyroxenes, probably because fewer of these two types of pyroxenes were analyzed. Pyroxenes of other Antarctic shergottites commonly display Ce anomalies (negative and positive; *e.g.*, WADHWA *et al.*, 1994) which are caused by REE mobilization in the Antarctic weather-

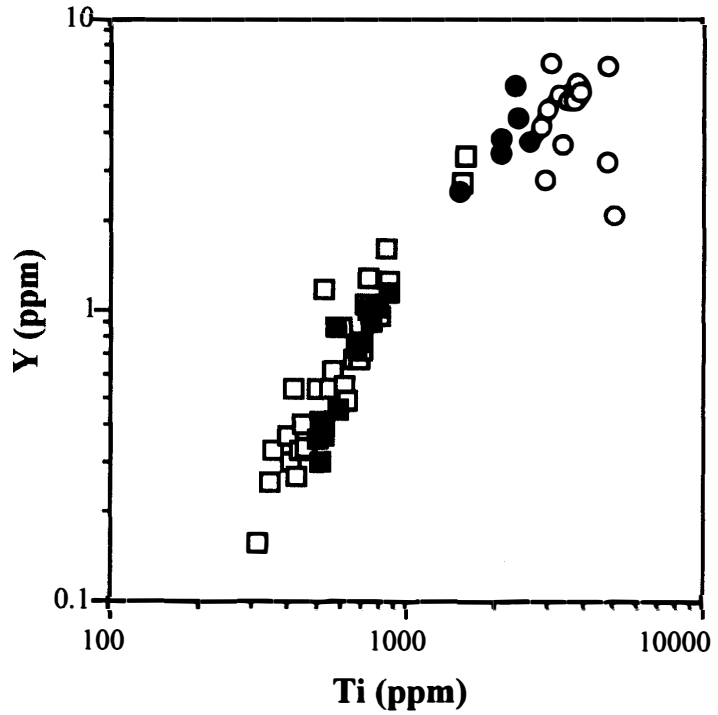

Fig. 7. Y versus Ti concentrations in low-Ca pyroxenes of Y79 (filled symbols) and ALH (open symbols). Squares represent poikilitic pyroxenes and circles non-poikilitic pyroxenes.

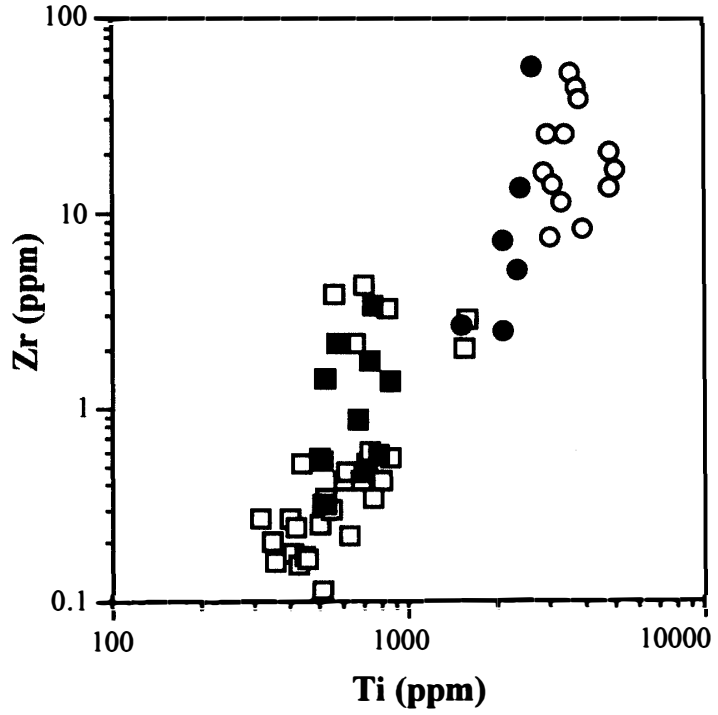

Fig. 8. Zr versus Ti concentrations in low-Ca pyroxenes of Y79 (filled symbols) and ALH (open symbols). Squares represent poikilitic pyroxenes and circles non-poikilitic pyroxenes.

ing environment (FLOSS and CROZAZ, 1991).

Figures 7 and 8 respectively show Y and Zr abundances *vs.* Ti concentrations in low-Ca pyroxenes, both poikilitic and non-poikilitic, of Y79 as well as ALH (HARVEY *et al.*, 1993). It is evident that trace and minor element abundances in pyroxenes of Y79 and ALH are similar.

4. Discussion

Because there are only rather subtle compositional differences (HARVEY *et al.*, 1993; TREIMAN *et al.*, 1994) between the two other lherzolites, ALH and the 13 g LEW88516 (LEW) for which less extensive data are available, we will, in the following discussion, emphasize mainly similarities and differences between Y79 and ALH.

4.1. Implications of major and minor element zoning in olivines and pyroxenes of Y79

In view of the high diffusivity of Fe and Mg in olivine, the fact that this zoning is preserved at all in this mineral suggests that Y79 could not have undergone extensive sub-solidus equilibration. It is noted that such zoning is not observed in olivines of ALH and LEW, which have uniform major element compositions (*e.g.*, HARVEY *et al.*, 1993). There is no apparent correlation between the composition of olivine crystals and the pyroxene immediately surrounding each crystal. This suggests that olivines crystallized prior to pyroxenes, and were incorporated in the growing pyroxene crystals. In fact, the rounded texture of the olivine crystals suggests that they have been partially resorbed prior to incorporation with the pyroxene, as if they were in a reaction relationship with the melt.

As noted earlier, even though the smooth zoning pattern in the large poikilitic pyroxene appears to be disturbed around the enclosed olivines, the distributions of major and minor elements in these "irregular" patches are similar to those in the smoothly zoned regions of these poikilitic pyroxenes. In fact, it is clear from Fig. 4 that there is no significant difference in Ti *vs.* Al systematics between the irregular patches and the smoothly zoned portions of the large poikilitic crystal. Similarities in zoning patterns for both major and minor elements suggest that, despite their irregular shapes, these patches are nevertheless similar in origin to the smoothly zoned regions, and are thus probably primary igneous features. We interpret the presence of these irregular pyroxene regions as indicating crystallization of pyroxene from a small volume of liquid around the olivines at the time they were trapped in the large pyroxene crystal.

4.2. REE in the three martian lherzolites

In all other SNC meteorites studied so far, with the exception of ALHA84001, the main REE carrier is calcium phosphate, either merrillite or apatite (WADHWA *et al.*, 1994; WADHWA and CROZAZ, 1995, 1998). Therefore, we would expect Ca-phosphate to be the main REE carrier in Y79 as well. However, like other investigators before of us, and despite extensive mapping with the electron microprobe, we were unable to locate any grains of merrillite or apatite in our thin section of Y79. The lack of detection of this mineral does not mean that it was never present in this meteorite. As in the case of the other two lherzolitic shergottites, Ca-phosphate in Y79 is most likely

heterogeneously distributed and occurs only in the non-poikilitic lithology. Therefore, it is possible that the thin sections studied so far by us and other workers (which all appear to be dominated by the poikilitic lithology) are lacking in this mineral. Alternatively, igneous calcium phosphate in Y79 may be less abundant than in the other lherzolitic shergottites due to loss by dissolution during terrestrial weathering; this suggestion is consistent with the occurrence of "partly decomposed" Ca phosphate grains in chips of Y79 (MITTLEFEHLDT *et al.* (1997, Fig. 1D). In ALH and LEW, merrillite is the mineral with the highest REE abundances and its REE pattern is essentially flat from La to Pr, then increases smoothly, has a small negative Eu anomaly, and finally slightly decreases from Gd to Lu (LUNDBERG *et al.*, 1990; HARVEY *et al.*, 1993). There is no reason to believe that the REE pattern of Y79's calcium phosphate would be any different, although we were not able to locate, and thus analyze, any phosphate grain in this meteorite. The reasons for this assertion are indirect but convincing.

Since merrillite is the main REE carrier in the shergottites (WADHWA *et al.*, 1994), if this mineral in Y79, ALH, and LEW has the same REE pattern, we would expect the whole rock patterns to be essentially identical. And, indeed, this appears to be the case. EBIHARA *et al.* (1997), MITTLEFEHLDT *et al.* (1997), and WARREN and KALLEMEYN (1997) all reported that the range of REE abundances in different samples of Y79 generally overlap those measured in ALH and LEW. Variations in absolute REE abundances in various aliquots of the same lherzolite are largely explained by the heterogeneous distribution of calcium phosphate, which dominates the REE budget in ALH and LEW. However, EBIHARA *et al.* (1997) noted that their ICPMS analyses of Y79 whole rocks are somewhat more LREE-depleted compared to those of ALH. Additionally, WARREN and KALLEMEYN (1997) also found their Y79 sample to be slightly depleted in La relative to the average of all bulk analyses of the three lherzolitic shergottites.

We performed simple mixing calculations, results of which are shown in Fig. 9, to better understand the cause of the variations in the REE abundances of measured Y79 bulk samples. We assume that, to first order, the bulk REE composition of Y79 is defined by three components, *i.e.*, (I) a REE-rich mineral having the same composition as that of merrillite in ALH (taken from HARVEY *et al.*, 1993), (II) a LREE-depleted component which is composed mostly of poikilitic pigeonite, but also contains smaller amounts of poikilitic augite as well as non-poikilitic pyroxenes (taken as the average composition of the Y79 pigeonites analyzed by us), and (III) a REE-poor component that is comprised mainly of olivine, but also other minerals found in lesser abundance such as maskelynite and opaque phases (the total REE contents of which are taken to be negligible). Figure 9 shows the results of three calculations (indicated by a solid thick line, a solid thin line and a dashed line) made using different proportions of components I, II and III; for comparison, Y79 bulk rock data from WARREN and KALLEMEYN (1997) (solid squares) and EBIHARA *et al.* (1997) (solid triangles) are also shown. Note that the results of the two calculations shown by the solid lines (mainly characterized by a variation in component I, *i.e.*, merrillite) can successfully reproduce the middle and heavy REE (Sm to Yb) abundances in the bulk rock data of WARREN and KALLEYMEYN (1997) and EBIHARA *et al.* (1997). However, these two calculations overestimate the

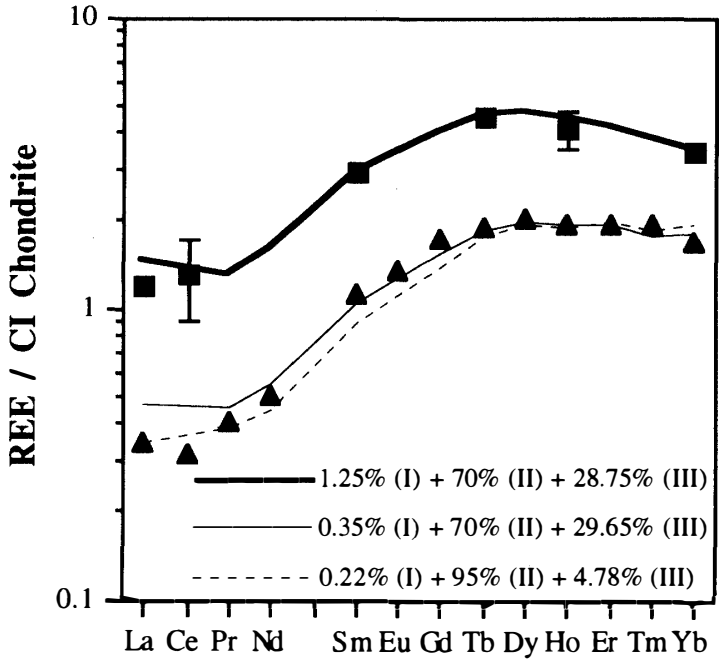

Fig. 9. Results of calculations to reproduce the REE abundances measured in Y79 bulk samples by mixing three end member components I, II and III; see text for details. Solid squares and triangles respectively show the bulk rock data of WARREN and KALLEMEYN (1997) and EBIHARA et al. (1997).

LREE (particularly La) concentrations. The third calculation (the dashed line in Fig. 9) illustrates that the apparent LREE depletion in the Y79 bulk samples may be due to an enrichment in the LREE-depleted component II (mostly poikilitic pigeonite). However, although an enrichment of component II can indeed produce the LREE depletion evident in the bulk data of EBIHARA *et al.* (1997), it is not as successful at reproducing the abundances of the middle REEs (particularly Nd to Tb). This, however, may be an artifact of the simple approximations made in assuming the compositions of the end member components. Thus, overall, variations of REE concentrations in whole rock samples can satisfactorily be accounted for by different proportions of the three components used in the mixing calculations.

We note that the frequent occurrence of Ce anomalies in Y79 pyroxenes, as well as observations of numerous alteration phases and "partly decomposed" calcium phosphates (MITTLEFEHLDT *et al.*, 1997), are consistent with extensive weathering of this meteorite while it resided in Antarctica. Still, despite this alteration, the REEs appear to be mobilized (if at all) only over small (*i.e.*, μm- to mm-scale) distances, such that bulk concentrations of REEs remain largely unaffected. We conclude that all three lherzolites have similar REE abundances and that differences in previously reported whole rock analyses (EBIHARA *et al.*, 1997; MITTLEFEHLDT *et al.*, 1997; WARREN and KALLEMEYN, 1997) are due to sample heterogeneity.

4.3. Similarities between Y-793605 and other lherzolitic shergottites

In addition to the REE abundances and the many textural, petrologic, and chemical

similarities between Y79 and the other two lherzolites already reported (EBIHARA *et al.*, 1997; IKEDA, 1997; MIKOUCHI and MIYAMOTO, 1997; MITTLEFEHLDT *et al.*, 1997; WARREN and KALLEMEYN, 1997), there is yet additional compositional evidence that supports a close association between these three meteorites.

Practically all elemental abundances for olivine, plagioclase, and pyroxene reported here for Y79 are indistinguishable from equivalent data for ALH and LEW and the same chemical zoning patterns are observed in the pyroxene of all three meteorites. The only exception may be an indication that the REE patterns of the low-Ca poikilitic pyroxenes of Y79 (CI-normalized Tm/La $<$ 40) are less steep than those of ALH (CI-normalized Tm/La ~ 40–60). However, the lower HREE/LREE ratio in these Y79 pyroxenes could also be attributed to calcium phosphate weathering and dissolution which locally remobilized REE, some of which may have been transported to these pyroxenes, thus lowering the Tm/La ratio in this mineral. REE transport and mobilization in Y79 pyroxene was likely facilitated by the intricate micro-crack network in this mineral (a feature commonly observed in other shergottites as well), which was most likely produced by the intense shock suffered by this meteorite during the impact that launched this sample from Mars.

Impressed by all the similarities between martian lherzolites and noting that peridotitic portions of layered terrestrial intrusions typically feature systematic heterogeneity down to cm-scales, WARREN and KALLEMEYN (1997) suggested that martian lherzolites are derived not only from a single layered intrusion, but from the same small region in the intrusion. If this is the case, we expect the three lherzolites to have identical cosmic ray exposure ages. And, indeed, the evidence (EUGSTER and POLNAU, 1997) points in that direction, although uncertainties on cosmic ray exposure ages are relatively large (4.4 $\pm$ 1.0 Ma) and NISHIIZUMI and CAFFEE (1997) could not "completely eliminate the possibility of a short pre-irradiation (of Y79) in the surface of the parent body."

In addition, since each of the three lherzolites was collected from a different ice field in Antarctica, it is unlikely that they are paired (*i.e.*, are fragments from the same fall). This was confirmed by NISHIIZUMI and CAFFEE (1997) who measured the ^{36}Cl concentrations in all three meteorites and concluded that the terrestrial age of ALH (210 $\pm$ 80 Ka) is significantly longer than those of the other two meteorites ($<$ 70 Ka). This situation is analogous to that of the three nakhlites (Nakhla, Lafayette, and Governador Valadares). Although these fell in different regions of the world, they exhibit striking petrographic and geochemical similarities and have the same exposure age of ~ 11 Ma (as reported in SCHULTZ and KRUSE, 1978) which led HARVEY and MCSWEEN (1992) and WADHWA and CROZAZ (1995) to suggest that all nakhlites could have originated from within the same lithologic unit on Mars.

4.4. Petrogenesis of the three martian lherzolites

In HARVEY *et al.* (1993), we outlined a model for the formation of ALH and LEW that can now be applied to Y79, as also done by MIKOUCHI and MIYAMOTO (1997). After initial crystallization of olivine and chromite, low-Ca pyroxene formed and enclosed the cumulus phases. The coherent trends for trace and minor elements in pyroxenes are consistent with progressive fractional crystallization from a single magma

reservoir. Continued crystallization included the onset of augite and then plagioclase formation, followed by more evolved phases such as merrillite. Finally, some reequilibration of major elements in the cumulus phases occurred, although preservation of zoning within individual olivine crystals in Y79 suggests that this reequilibration was not extensive, at least in this sample. If these three lherzolitic shergottites did indeed originate from the same lithologic unit on Mars (as indicated above in Section 4.3), the preservation of major element zoning in Y79 olivines may indicate that this sample crystallized at a shallower depth (relative to ALH and LEW) in this lithologic unit.

The lherzolite parent melt compositions were LREE-depleted (LUNDBERG *et al.*, 1990; HARVEY *et al.*, 1993). For Y79, as for the other two lherzolites, this can be inferred both by "inverting" the core low-Ca pyroxene composition and from the REE pattern of the glassy region of the melt inclusion in the poikilitically enclosed olivine. As shown in Fig. 5, the latter is LREE-depleted and parallel to the REE pattern of the Y79 whole rock. This is expected if Y79 consists of a cumulate portion (that contains only a small fraction of the overall REE budget of this rock) and a trapped melt component (with the composition of the parent melt) that essentially crystallized as a closed system. The REE composition of the glass in the melt inclusion, thus, approximately reflects the composition of the parent melt of Y79. This indicates that, like those of other shergottites, the parent magma of Y79 was derived by partial melting of an already depleted martian mantle.

5. Conclusions

(1) Major, minor and trace element abundances in individual grains of maskelynite, olivine, glassy melt inclusion, and pyroxene show striking similarities, including zoning patterns in pyroxene, to those in other lherzolitic shergottites.

(2) The common occurrence of Ce anomalies in low-Ca pyroxenes indicates that severe weathering occurred after Y79 fell in Antarctica. Weathering in the Antarctic may have been responsible for the dissolution of calcium phosphate (as previously noted by MITTLEFEHLDT *et al.*, 1997) and localized mobilization of REEs.

(3) Variations in the absolute REE abundances between various whole rock measurements of all three lherzolites can be largely accounted for by heterogeneity in the distribution of merrillite. Additionally, the LREE depletion noted in several bulk samples of Y79 may be due to an enrichment of poikilitic pyroxene.

(4) The data presented here are consistent with the view that all martian lherzolites may have come from the same lithologic unit within a single layered intrusion. However, unlike ALH and LEW, some olivines of Y79 have retained major element zonation suggesting that this sample did not undergo significant sub-solidus reequilibration, and may have originated at a shallower depth in this lithologic unit than ALH and LEW.

(5) The magma from which these cumulates formed was derived by partial melting of already depleted material and fractional crystallization in a closed system played an important role in the formation of these meteorites.

Acknowledgments

We would like to thank the National Institute of Polar Research (NIPR) for providing a sample of Y-793605, as well as H. KOJIMA, P. WARREN, M. MIYAMOTO, and K. YANAI who organized the consortium to study this meteorite. The constructive comments and suggestions of two anonymous reviewers are much appreciated. This work was funded by NASA grants NAG5-4326 to MW, NAGW-3371 to GC, and RTOP 344-31-20-23 to GM.

References

EBIHARA, M. and ANDERS, E. (1982): Solar system abundances of the elements. Geochim. Cosmochim. Acta, **46**, 2363–2380.

EBIHARA, M., KONG, P. and SHINOTSUKA, K. (1997): Chemical composition of Y-793605, a martian lherzolite. Antarct. Meteorite Res., **10**, 83–94.

EUGSTER, O. and POLNAU, E. (1997): Mars-Earth transfer time of lherzolite Yamato-793605. Antarct. Meteorite Res., **10**, 143–149.

FLOSS, C. and CROZAZ, G. (1991): Ce anomalies in LEW85300 eucrite: Evidence for REE mobilization during Antarctic weathering. Earth Planet. Sci. Lett., **107**, 13–24.

GRADY, M.M., VERCHOVSKY, A.B., WRIGHT, I.P. and PILLINGER, C.T. (1997): The light element geochemistry of Yamato-793605. Antarct. Meteorite Res., **10**, 151–162.

HARVEY, R.P. and MCSWEEN, H.Y., Jr. (1992): Petrogenesis of the nakhlite meteorites: Evidence from cumulate mineral zoning. Geochim. Cosmochim. Acta, **56**, 1655–1663.

HARVEY, R.P., WADHWA, M., MCSWEEN, H.Y., Jr. and CROZAZ, G. (1993): Petrography, mineral chemistry, and petrogenesis of Antarctic shergottite LEW88516. Geochim. Cosmochim. Acta, **57**, 4769–4783.

IKEDA, Y. (1997): Petrology and mineralogy of the Y-793605 martian meteorite. Antarct. Meteorite Res., **10**, 13–40.

KOJIMA, H., MIYAMOTO, M. and WARREN, P.H. (1997): The Yamato-793605 martian meteorite consortium. Antarct. Meteorite Res., **10**, 3–12.

LUNDBERG, L.L., CROZAZ, G., MCKAY, G. and ZINNER, E. (1988): Rare earth element carriers in the Shergotty meteorite and implications for its chronology. Geochim. Cosmochim. Acta, **52**, 2147–2163.

LUNDBERG, L.L., CROZAZ, G. and MCSWEEN, H.Y., Jr. (1990): Rare earth elements in minerals of the ALHA 77005 shergottite and implications for its parent magma and crystallization history. Geochim. Cosmochim. Acta, **54**, 2535–2547.

MAYEDA, T.K., YANAI, K. and CLAYTON, R.N. (1995): Another martian meteorite. Lunar and Planetary Science XXVI. Houston, Lunar Planet. Inst., 917–918.

MCSWEEN, H.Y., Jr. (1994): What we have learned about Mars from SNC meteorites. Meteoritics, **29**, 757–779.

MIKOUCHI, T. and MIYAMOTO, M. (1996): A new member of lherzolitic shergottite from Japanese Antarctic meteorite collection: Mineralogy and petrology of Yamato-793605. Antarctic Meteorites XXI. Tokyo, Natl Inst. Polar Res., 104–106.

MIKOUCHI, T. and MIYAMOTO, M. (1997): Yamato-793605: A new lherzolitic shergottite from the Japanese Antarctic meteorite collection. Antarct. Meteorite Res., **10**, 41–60.

MISAWA, K., NAKAMURA, N., PREMO, W.R. and TATSUMOTO, M. (1997): U-Th-Pb isotopic systematics of lherzolitic shergottite Yamato-793605. Antarct. Meteorite Res., **10**, 95–108.

MITTLEFEHLDT, D.W., WENTWORTH, S.J., WANG, M.-S., LINDSTROM, M.M. and LIPSCHUTZ, M.E. (1997): Geochemistry of and alterations phases in martian lherzolite Y-793605. Antarct. Meteorite Res., **10**, 109–124.

NAGAO, K., NAKAMURA, T., MIURA, Y.N. and TAKAOKA, N. (1997): Noble gases and mineralogy of primary igneous materials of the Yamato-793605 shergottite. Antarct. Meteorite Res., **10**, 125–142.

NISHIIZUMI, K. and CAFFEE, M.W. (1997): Exposure history of shergottite Yamato 793605. Antarctic Meteorites XXII. Tokyo, Natl Inst. Polar Res., 149–151.

SCHULTZ, L. and KRUSE, H. (1978): Light noble gases in stony meteorites —A compilation. Nucl. Track Detection, **2**, 65–103.

SMITH, M.R., LAUL, J.C., MA, M.-S., HUSTON, T., VERKOUTEREN, R.M., LIPSCHUTZ, M.E. and SCHMITT, R. A. (1984): Petrogenesis of the SNC (shergottites, nakhlites, chassignites) meteorites: Implications for their origin from a large dynamic planet, possibly Mars. Proc. Lunar Planet. Sci. Conf., 14th, Pt. 2, B612–B630 (J. Geophys. Res., **89** Suppl.).

TREIMAN, A.H., MCKAY, G.A., BOGARD, D.D., MITTLEFEHLDT, D.W., WANG, M.-S., KELLER, L., LIPSCHUTZ, M.E., LINDSTROM, M.M. and GARRISON, D. (1994): Comparison of the LEW88516 and ALHA77005 martian meteorites: Similar but distinct. Meteoritics, **29**, 581–592.

WADHWA, M. and CROZAZ, G. (1995): Trace and minor elements in minerals of nakhlites and Chassigny: Clues to their petrogenesis. Geochim. Cosmochim. Acta, **59**, 3629–3645.

WADHWA, M. and CROZAZ, G. (1998): The igneous crystallization history of an ancient martian meteorite from rare earth element microdistributions. Meteorit. Planet. Sci., **33**, 685–692.

WADHWA, M., MCSWEEN, H.Y., Jr. and CROZAZ, G. (1994): Petrogenesis of shergottite meteorites inferred from minor and trace element microdistributions. Geochim. Cosmochim. Acta, **58**, 4213–4229.

WARREN, P.H. and KALLEMEYN, G.W. (1997): Yamato-793605, EET79001, and other presumed martian meteorites: Compositional clues to their origins. Antarct. Meteorite Res., **10**, 61–81.

YANAI, K. (1995): Re-searching for martian rocks from diogenite-diogenitic achondrites. Lunar and Planetary Science XXVI. Houston, Lunar Planet. Inst., 1533–1534.

ZINNER, E. and CROZAZ, G. (1986): A method for the quantitative measurement of rare earth elements in the ion microprobe. Intl. J. Mass. Spectrom. Ion Proc., **69**, 17–38.

(Received October 20, 1998; Revised manuscript accepted January 28, 1999)